SiliconPV 2025, 15th International Conference on Crystalline Silicon Photovoltaics

Advances in Industrial Silicon Solar Cells

https://doi.org/10.52825/siliconpv.v3i.2681

Published: 13 Jan. 2025

Numerical Simulation of Flexible Silicon Heterojunction Solar Cell with 27.2% Efficiency

Deep Shikha[1,*] and Sayak Bhattacharya[1,2]

[1]Department of ECE, Indraprastha Institute of Information Technology Delhi, India

[2]Centre for Quantum Technology, Indraprastha Institute of Information Technology Delhi, India

*Correspondence: Deep Shikha, deeps@iiitd.ac.in

Abstract. In this article, we numerically demonstrate 27.2% power conversion efficiency in a 15µm-thick, flexible photonic crystal (PhC) silicon heterojunction cell (SHJ). This new class of SHJ cell combines the superior electronic performance of hetero-junction contacts with the wave interference-based light-trapping capability of thin-film silicon PhC, surpassing the traditional Lambertian limit. Through numerical simulations, we show that our flexible PhC-SHJ cell is capable of achieving a short-circuit current density of 44.31mA/cm^2 and an open circuit voltage of 756.8mV, paving the way for flexible photovoltaic technology with efficiency beyond 27%.

Keywords: Flexible Photovoltaic, Solar Cell, Hetero-Junction, Photonic Crystal

1. Introduction

Silicon, despite being an indirect bandgap semiconductor, remains the most widely used material in solar cells due to its abundance, well-established fabrication process, and non-toxicity. However crystalline silicon (c-Si) solar cells are typically inflexible and susceptible to bulk recombination [1]-[2] as more than 100µm-thick silicon is required for significant solar absorption due to the indirect bandgap nature of c-Si.

In response to the need for flexible solar cells, the development of thin-film photovoltaic (TFPV) technologies has gained momentum. Materials like Gallium Arsenide (GaAs), Copper Indium Gallium Selenide (CIGS), and Perovskites have been explored, but they often face challenges such as scarcity of raw materials, toxicity, slow production rates, and instability. One promising approach is the use of photonic crystal (PhC) c-Si solar cells that employ wave-interference based slow-light modes to trap sunlight [3]. In contrast to traditional solar cells, PhC c-Si solar cells have shown the ability to absorb solar energy beyond the statistical ray-optics based Lambertian limit [4]. This ability allows thin, flexible PhC cells to absorb as much light as much thicker silicon cells, providing advantages such as flexibility, lower bulk recombination, and reduced costs due to thinner silicon layer.

A critical area of photovoltaics research focuses on improving charge carrier transport. In c-Si solar cells, a significant amount of charge-carrier recombination occurs at the interface between the silicon and the contacts. To mitigate this, advancements have been made in contact technologies, including the shift from passivated emitter and rear cell (PERC) to tunnel oxide passivated contact (TOPCon) and silicon heterojunction (SHJ) solar cells [5]-[7]. Among these, SHJ solar cells have garnered significant attention for their potential to improve efficiency. SHJ cells typically use hydrogenated amorphous silicon (a-Si:H) layers as electron-selective and hole-selective contacts, with an intrinsic a-Si:H layer providing superior chemical passivation [8]. These structures offer better field passivation and reduced energy barriers

when in contact with transparent conducting oxides (TCOs). However, doped a-Si:H layers suffer from limitations such as low electrical conductivity and high activation energy, hindering their performance.

This paper proposes a hybrid approach, combining flexible photonic crystal-based light trapping with SHJ cell technology, to improve the performance of solar cells. The architecture of the flexible PhC-SHJ cell is presented in sec. 2. The numerical simulations in sec. 3 indicate that a 15μm, flexible PhC-SHJ cell can achieve a power conversion efficiency of 27.2%. With further optimization, this new class of SHJ cells has the potential to exceed the efficiency records.

2. Solar Cell Design with Numerical Details

The schematic of the 2D cross-section of our proposed flexible c-Si heterojunction solar cell is shown in *Figure 1*. It consists of a 15 micron-thick, n-type c-Si with resistivity of 5 Ω-cm. The front surface of the c-Si is textured with a square lattice of inverted pyramids of lattice constant of 3 micron. The side-wall angle of the inverted pyramids are 54.7 degrees, same as the angle between the (111) and (100) planes of c-Si. Such pyramids can be wet-etched on the c-Si surface using KOH etching. The lattice constant and the side-wall angle fix the height of the pyramids to 2.12 micron.

The top surface of the cell features a dual-layer antireflection coating (ARC) that consists of 100 nm SiO_2 layer at the top and 45 nm SiC layer between the SiO_2 and c-Si. The details of the light-trapping in this photonic crystal are described in [3]. An intrinsic hydrogenated amorphous Si (i-a-Si:H) layer of 3.5 nm thickness is placed between the c-Si layer and front/back contacts. p-doped a-Si:H (p-a-Si:H) and n-doped a-Si:H (n-a-Si:H) of thicknesses 6 nm and 20 nm are deposited on the i-a-Si:H at the front electrode and back surface, respectively. Transparent conductive oxide (TCO) layers of 150 nm (ITO- Indium tin oxide) with free carrier density of 6.5×10^{19} cm^{-3} and 70 nm with free carrier density of 2×10^{20} cm^{-3} are placed at the back and front contacts, respectively [9]-[11].

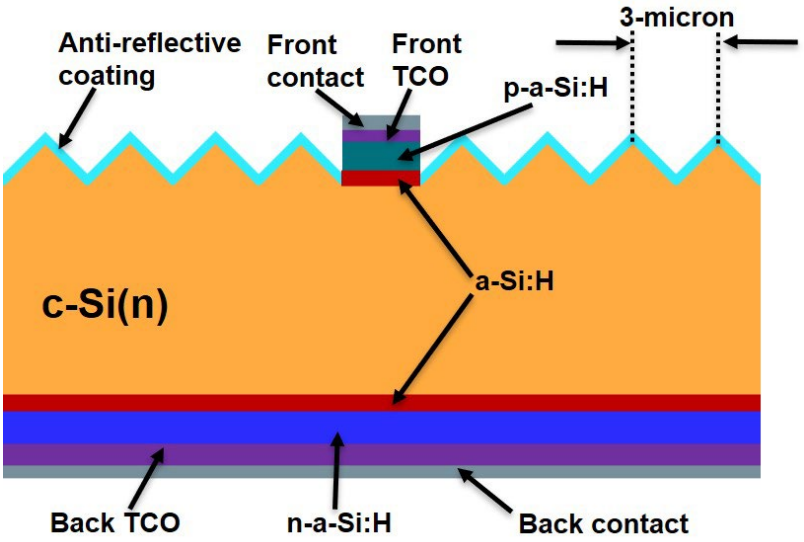

Figure 1. *Schematic of the proposed PhC c-SHJ flexible solar cell. The cell consists of n-type bulk with a thin layer of a-Si:H and doped a-Si:H layer below the metal contacts with a TCO layer. The front surface shows the PhC structure with anti-reflective coatings*

The carrier transport calculations are performed using Quokka [6],[7]. All the simulations are done at 300K. The physical models and parameters corresponding to crystalline silicon, defect densities and effective density of states of intrinsic and doped hydrogenated amorphous

silicon are the same as [9],[12],[13] (see *Table 1*). The injection-dependent recombination parameter (J_0) of the amorphous silicon-hydrogenated (a-Si:H) boundaries are given by:

$$J_{0,\,front} = 0.3826 \times 10^{[1.367+0.7028\cos(\log(\Delta p))]} + 0.2459\sin(\log(\Delta p)) - 0.04068\cos(2\log(\Delta p)) - 0.2271\sin(2\log(\Delta p)). \quad (1)$$

$$J_{0,\,back} = 0.3826 \times 10^{[1.029+0.293\cos(1.304\log(\Delta n))]} - 0.5323\sin(1.304\log(\Delta n)) + 0.01279\cos(2.608\log(\Delta n)) + 0.1621\sin(2.608\log(\Delta n)). \quad (2)$$

where, $\Delta p(cm^{-3})$ and $\Delta n(cm^{-3})$ represents the excess densities of holes and electrons at front and back contact boundaries, respectively.

Table 1. *Simulation input parameters used in modelling the bulk properties of c-Si wafer and a-Si:H layers as described in [9][12][13]. All the parameters are calculated from conduction band (CB) and valence band (VB) edges.*

Parameters	a-Si:H(i)	a-Si:H(n)	a-Si:H(p)
Layer thickness (mm)	0.0035	0.02	0.006
Mobility gap (eV)	1.75	1.80	1.75
Effective DOS in CB and VB	2×10^{20}	2×10^{20}	2×10^{20}
Urbach energy (VB tail) (eV)	0.045	0.05	0.05
Urbach energy (CB tail) (eV)	0.03	0.03	0.03
Electron mobility ($cm^2V^{-1}s^{-1}$)	25	20	25
Hole mobility ($cm^2V^{-1}s^{-1}$)	5	4	5
Gaussian defect density (cm^{-3})	9×10^{16}	2.75×10^{19}	2.63×10^{19}
Gaussian donor peak position from VB (eV)	0.83	0.50	1.00
Gaussian acceptor peak position from VB (eV)	1.08	0.7	1.20
Neutral σ (for Urbach tail and Gaussian Defects) (cm^2)	10^{-19}	6.5×10^{-16}	6.5×10^{-16}
Charged σ (for Urbach tail and Gaussian Defects) (cm^2)	10^{-18}	6.5×10^{-15}	6.5×10^{-15}
Activation energy (eV)	0.83	0.20	0.20
Correlation energy (eV)	0.18	0.20	0.18

3. Key Results

Figure 2 shows the J-V and P-V characteristics of the 15µm PhC-SHJ cell. The reduced surface recombination due to the superior performance of the a-Si:H-p/n-a-Si:H- TCO stack enables a V_{OC} of 756.8mV while the wave-interference based light-trapping in thin-film PhC leads to a J_{SC} of 44.31mA/cm^2. Overall, the proposed c-Si PhC-SHJ solar cell is numerically shown to have a power conversion efficiency of 27.2%.

Different loss pathways associated with the 15µm PhC-SHJ cell are quantified in *Figure 3* using free energy loss analysis (FELA) [14]-[15] module of Quokka. Out of the total generated power density of 29.92mW/cm^2 at the maximum power point (MPP), 1.21mW/cm^2 and 1.5mW/cm^2 are attributed to the resistive loss and recombination loss, respectively. This leads to an output power density of 27.21mW/cm^2 at the MPP.

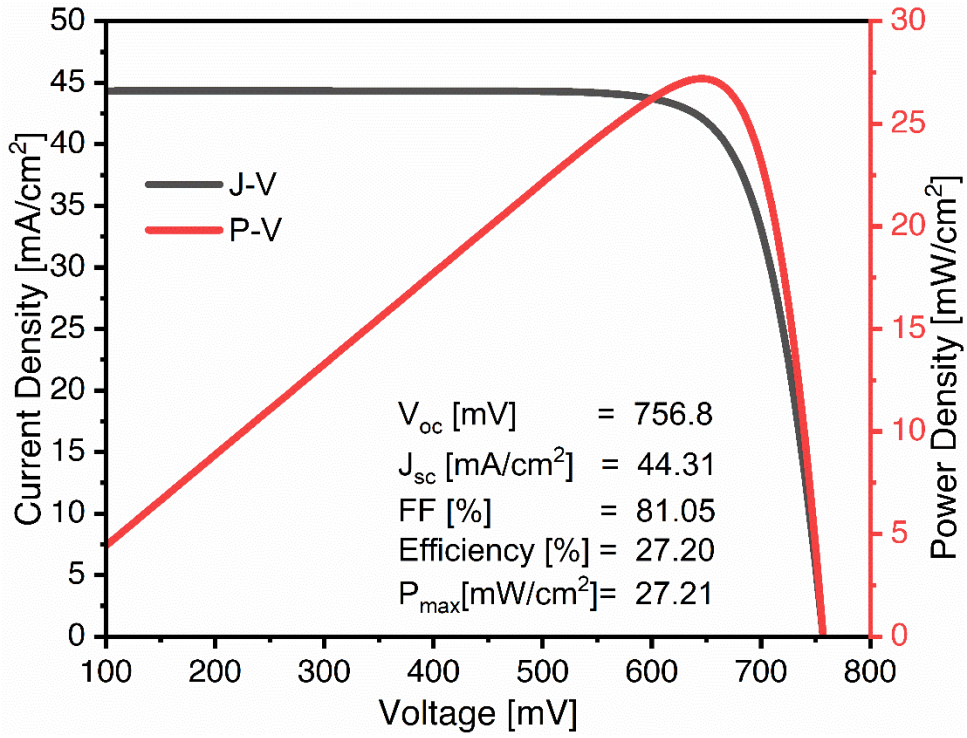

Figure 2. *J-V (black) and P-V (red) curves of our proposed 15μm thick Photonic crystal SHJ cell. In this simulation, we assume SRH lifetime = 10ms*

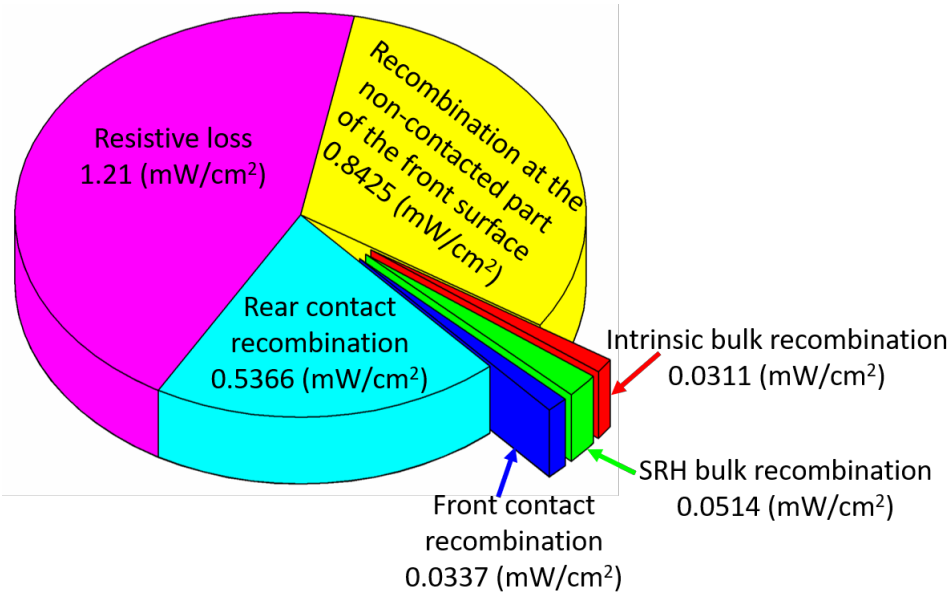

Figure 3. *Free energy loss analysis of PhC-SHJ Solar Cells*

Although SRH lifetime (τ_{SRH}) =10ms is achievable in high quality c-Si, this requirement is a potential source of significant manufacturing cost. Thus, a trade-off between cost and τ_{SRH} becomes crucial for mass-production. We analyze the performance of our PhC-SHJ cell over a range of 0.1-10ms SRH lifetime. *Figure 4* shows that the conversion efficiency improves by 0.2% going from 1.5ms to 10ms. Thus, a τ_{SRH} of 1.5ms would be sufficient to obtain a power conversion efficiency close to 27%. On the other hand, the efficiency shows a significant jump (2%) as τ_{SRH} improves from 0.1ms to 1ms. Further, the PhC-SHJ cell is capable of achieving 26% efficiency with τ_{SRH} =0.3ms.

In absence of shading, our 15µm thick inverted pyramid PhC cell yields a photo-current density of 44.39 mA/cm^2 out of the total available 46.36mA/cm^2 over the 300-1200 nm spectral range. Thus, the optical loss associated with imperfect light-trapping in the PhC is 4.25%. Another unavoidable source of optical loss in our cell is the front contact shading. A part of the incident sunlight is blocked by the front contact, leading to a reduction of the photo-current density. *Figure 5* shows that the J_{SC} linearly decreases from 44.39mA/cm^2 for no shading to 43.1mA/cm^2 for 50µm shading width. This corresponds to 0.85% reduction of conversion efficiency. In our study, we have considered the shading width to be 47% of the front-contact width [16].

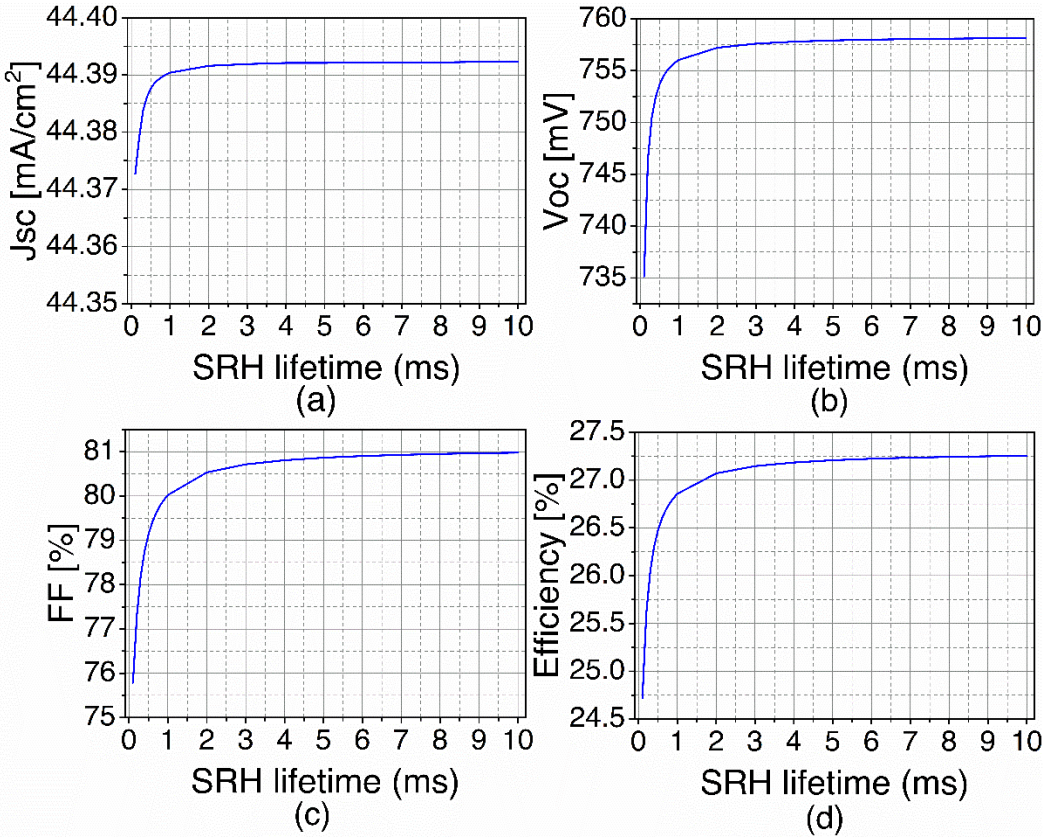

Figure 4. *Effect of SRH lifetime on the performance parameters of the 15micron-thick PhC-SHJ cell: the efficiency increases significantly as SRH lifetime improves from 0.1ms to 1ms. However, the efficiency saturates approximately beyond 1.5ms*

4. Conclusion

Our numerical investigation demonstrates a new class of flexible, thin-film cell that exploits the unprecedented light absorption in c-Si PhC and efficient electronic performance of heterojunction contact. In *Table 2*, we show a comparison of our flexible PhC-SHJ cell with other cells (described in [13]) that are at least 10-times thicker than the PhC-SHJ cell. The ease of fabrication of wavelength-scale inverted pyramid textures on the top of already existing SHJ structures provides a way to high-efficiency, flexible photovoltaic technology.

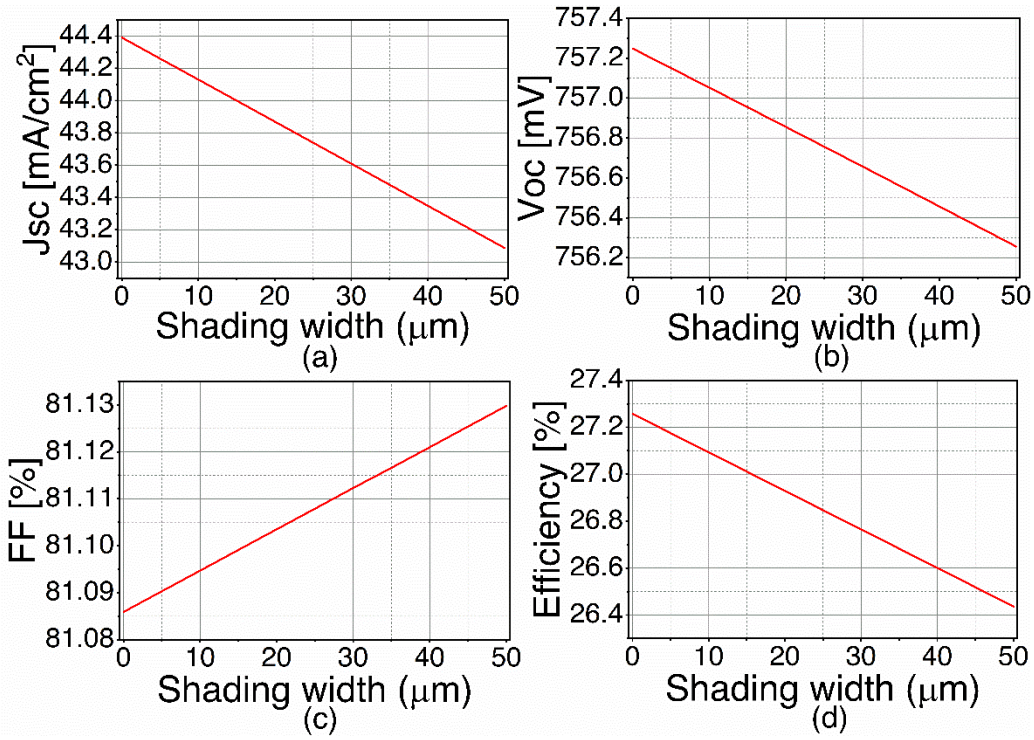

Figure 5. *Effect of shading width on PhC-SHJ solar cell. (a) The J_{SC} changes from 44.39mA/cm² for no shading width to 43.1mA/cm² for a maximum of 50mm shading width. (b) and (c) there is no significant change of V_{OC} and FF, and (d) the overall efficiency decreases by 0.85%*

Table 2. *Comparison of simulated and measured J-V Parameters of different cell types with our proposed PhC-SHJ Cell.*

Cell Type	V_{OC} (mV)	J_{SC} (mA/cm²)	FF (%)	η (%)
SHJ-simulated (our work)	756.8	44.31	81.05	27.2
HJT-simulated*	743	36.7	80.3	21.9
PERL-simulated*	710	42.3	82.6	24.8
n-Pasha-simulated*	656	39.5	79.8	20.7
IBC-simulated*	705	42.2	83.1	24.7
PERC-simulated*	655	39.8	79.4	20.7
PERL-measured*	706	42.7	82.8	25.0
IBC-measured*	703	42.0	82.7	24.4
n-Pasha-measured*	655	39.5	79.8	20.7

* All the data has been taken from [13].

Data availability statement

The data supporting the results of this contribution are available upon reasonable request from the corresponding author.

Author contributions

Deep Shikha: Conceptualization, Investigation, Visualization, Writing-original draft.

Sayak Bhattacharya: Supervision, Investigation, Writing- Review & Editing.

Competing interests

The authors declare no competing interests.

Funding and Acknowledgement

This work was supported in part by the Start-up Research Grant from Science and Engineering Research Board (SERB) India.

References

[1] H. Lin, M. Yang, X. Ru, G. Wang, S. Yin, F. Peng, C. Hong, M. Qu, J. Lu, L. Fang, C. Han, P. Procel, O. Isabella, P. Gao, Z. Li, and X. Xu, "Silicon heterojunction solar cells with up to 26.81% efficiency achieved by electrically optimized nanocrystalline-silicon hole contact layers," Nature Energy, vol. 8, pp. 789–799, Aug 2023. https://doi.org/10.1038/s41560-023-01255-2

[2] P. Wawer, J. Müller, M. Fischer, P. Engelhart, A. Mohr, and K. Petter, "Latest trends in development and manufacturing of industrial, crystalline silicon solar-cells," Energy Procedia, vol. 8, pp. 2–8, 2011. https://doi.org/10.1016/j.egypro.2011.06.093

[3] S. Bhattacharya and S. John, "Beyond 30% conversion efficiency in silicon solar cells: A numerical demonstration," Scientific Reports, vol. 9, Dec 2019. https://doi.org/10.1038/s41598-019-48981-w

[4] M. L. Hsieh, A. Kaiser, S. Bhattacharya, S. John, and S. Y. Lin, "Experimental demonstration of broadband solar absorption beyond the Lambertian limit in certain thin silicon photonic crystals," Scientific Reports, vol. 10, Dec 2020. https://doi.org/10.1038/s41598-020-68704-w

[5] K. Yoshikawa, H. Kawasaki, W. Yoshida, T. Irie, K. Konishi, K. Nakano, T. Uto, D. Adachi, M. Kanematsu, H. Uzu, and K. Yamamoto, "Silicon heterojunction solar cell with interdigitated back contacts for a photoconversion efficiency over 26%," Nature Energy, vol. 2, Mar 2017. https://doi.org/10.1038/nenergy.2017.32

[6] A. Richter, R. Müller, J. Benick, F. Feldmann, B. Steinhauser, C. Reichel, A. Fell, M. Bivour, M. Hermle, and S. W. Glunz, "Design rules for high-efficiency both-sides-contacted silicon solar cells with balanced charge carrier transport and recombination losses," Nature Energy, vol. 6, pp. 429–438, Apr 2021. https://doi.org/10.1038/s41560-021-00805-w

[7] B. Min, M. Müller, H. Wagner, G. Fischer, R. Brendel, P. P. Altermatt, and H. Neuhaus, "A roadmap toward 24% efficient perc solar cells in industrial mass production," IEEE Journal of Photovoltaics, vol. 7, no. 6, pp. 1541–1550, Nov 2017. https://doi.org/10.1109/JPHOTOV.2017.2749007

[8] S. W. Glunz, B. Steinhauser, J. I. Polzin, C. Luderer, B. Grübel, T. Niewelt, A. M. Okasha, M. Bories, H. Nagel, K. Krieg, F. Feldmann, A. Richter, M. Bivour, and M. Hermle, "Silicon-based passivating contacts: The TOPCon route," Progress in Photovoltaics: Research and Applications, vol. 31, pp. 341–359, Apr 2023. https://doi.org/10.1002/pip.3522

[9] Z. Peng and G. Ling, "Design, fabrication and characterization of thin-film materials for heterojunction silicon wafer solar cells," Thesis, 2014. [Online]. Available: https://www.researchgate.net/publication/276355293.

[10] D. Qiu, W. Duan, A. Lambertz, K. Bittkau, P. Steuter, Y. Liu, A. Gad, M. Pomaska, U. Rau, and K. Ding, "Front contact optimization for rear-junction SHJ solar cells with ultra-thin n-type nanocrystalline silicon oxide," Solar Energy Materials and Solar Cells, vol. 209, Jun 2020. https://doi.org/10.1016/j.solmat.2020.110471

[11] H. Nasser, F. Es, M. Z. Borra, E. Semiz, G. K¨okbudak, E. Orhan, and R. Turan, "On the application of hole-selective moox as full-area rear contact for industrial scale p-type c-si solar cells," Progress in Photovoltaics: Research and Applications, vol. 29, pp. 281–293, Mar 2021. https://doi.org/10.1002/pip.3363

[12] M. Taguchi, A. Yano, S. Tohoda, K. Matsuyama, Y. Nakamura, T. Nishiwaki, K. Fujita, and E. Maruyama, “24.7% record efficiency hit solar cell on thin silicon wafer,” IEEE Journal of Photovoltaics, vol. 4, pp. 96–99, Jan 2014. https://doi.org/10.1109/JPHOTOV.2013.2282737

[13] A. Fell, K. R. McIntosh, P. P. Altermatt, G. J. Janssen, R. Stangl, A. Ho-Baillie, H. Steinkemper, J. Greulich, M. Muller, B. Min, K. C. Fong, M. Hermle, I. G. Romijn, and M. D. Abbott, “Input parameters for the simulation of silicon solar cells in 2014,” IEEE Journal of Photovoltaics, vol. 5, pp. 1250–1263, Jul 2015. https://doi.org/10.1109/JPHOTOV.2015.2430016

[14] R. Brendel, S. Dreissigacker, N.-P. Harder, and P. P. Altermatt, “Theory of analyzing free energy losses in solar cells,” Applied Physics Letters, vol. 93, no. 17, p. 173503, Oct 2008. https://doi.org/10.1063/1.3006053.

[15] C. N. Kruse, K. Bothe, and R. Brendel, “Comparison of free energy loss analysis and synergistic efficiency gain analysis for perc solar cells,” IEEE Journal of Photovoltaics, vol. 8, no. 3, pp. 683–688, May 2018. 10.1109/JPHOTOV.2018.2802779

[16] R. Woehl, M. Hörteis, and S. W. Glunz, “Analysis of the optical properties of screen-printed and aerosol-printed and plated fingers of silicon solar cells,” Advances in OptoElectronics, vol. 2008, no. 1, p. 759340, Sep 2008. https://doi.org/10.1155/2008/759340